

"Decoherence in Combined Quantum Mechanical and Classical Mechanical Methods for Dynamics as Illustrated for Non-Born-Oppenheimer Trajectories," D. G. Truhlar, in *Quantum Dynamics of Complex Molecular Systems*, edited by D. A. Micha and I. Burghardt, Springer Series in Chemical Physics, Vol. 83 (Springer, Berlin, 2007), pp. 227-243. doi.org/10.1007/978-3-540-34460-5_9

Decoherence in Combined Quantum Mechanical and Classical Mechanical Methods for Dynamics as Illustrated for Non-Born–Oppenheimer Trajectories

Donald G. Truhlar

Summary. This chapter discusses the role of decoherence in mixed quantum–classical approaches to electronically nonadiabatic chemical dynamics. The correlation of electronic and nuclear motion, which is not included in the semiclassical Ehrenfest or time-dependent Hartree method, induces decoherence in the reduced electronic density matrix, and the chapter shows how this can be modeled by adding algorithmic demixing to the Liouville-von Neumann equation. The resulting mixed quantum–classical equations of motion involve stochastically controlled, smooth, and continuous surface switching coupled to coherent propagation through each region of strong interaction of the electronic states. The chapter also reviews test results that show good agreement with fully quantum mechanical results for a diverse set of atom–diatom test cases.

1 Introduction

The coupling of quantum mechanics to classical mechanics is a recurring theme in the treatment of complex systems because a full quantum mechanical treatment is usually possible only for simple systems. The coupling may occur in the generation of potential energy surfaces, as in combined quantum mechanical and molecular mechanical methods [1–3] or it may occur in the dynamics step, as when quantum mechanical nuclear-motion effects are combined with transition state theory or molecular dynamics simulations [2, 4–7]. Conventional molecular dynamics simulations themselves, even when the nuclear motion is only treated classically, involve using quantum mechanics, explicitly or implicitly, to derive the Born–Oppenheimer [8] potential energy surface and then treating nuclear motion classically [7, 9–12]. This kind of joining of the two mechanics raises fewer theoretical questions than the first two. However, if we allow for Born–Oppenheimer breakdown, that is, electronic nonadiabaticity, then a number of conceptual issues arise [7, 13–31]. Very similar issues arise in Born–Oppenheimer processes if some nuclear degrees of freedom are treated quantum mechanically and others classically [32–41]. The present article is

concerned with this problem and especially with elucidating the important role of decoherence in shaping a physically correct form for the equations of motion of the quantal and classical subsystems. Furthermore we seek a practical algorithm that allows us to simulate systems in which decoherence plays an important role. Although one could illustrate the theory by any problem in which some degrees of freedom are treated as quantal but are not simply adiabatic and other degrees of freedom are treated as classical, we use the problem of electronic nonadiabaticity as our illustrative example, with all nuclear degrees of freedom classical. Furthermore, we start with a Hartree approximation (also called the Ehrenfest approximation [14, 21], the time-dependent self-consistent-field approximation [20, 37, 40], or the self-consistent eikonal approximation [15]), which assumes only a mean-field (uncorrelated) coupling of the electronic and nuclear degrees of freedom, and we show how adding correlation effects leads to decoherence. Since the nuclear degrees of freedom are coupled to the electronic ones, we will see that they require some quantum mechanical elements for their description.

2 Theory

The quantum mechanical time-dependent Hartree approximation for coupled electronic and nuclear motion is

$$\Psi = \phi^{\text{elec}}(\mathbf{r}, t) \psi^{\text{nuc}}(\mathbf{R}, t). \quad (1)$$

The factors in (2) satisfy an electronic mean-field Schrödinger equation

$$i\hbar \frac{\partial}{\partial t} \phi^{\text{elec}} = \langle \psi^{\text{nuc}} | H | \psi^{\text{nuc}} \rangle_{\mathbf{R}} \phi^{\text{elec}}(\mathbf{R}, t) \quad (2)$$

and a nuclear mean-field Schrödinger equation

$$i\hbar \frac{\partial}{\partial t} \psi^{\text{nuc}} = \left\langle \psi^{\text{elec}} | H | \psi^{\text{elec}} \right\rangle_{\mathbf{r}} \psi^{\text{nuc}}(\mathbf{R}, t), \quad (3)$$

where $i = \sqrt{-1}$, \hbar is Planck's constant divided by 2π , \mathbf{r} and \mathbf{R} denote the electronic and nuclear coordinates, respectively, and t is time.

Now we approximate ψ^{nuc} by an ensemble of trajectories, which yields a semiclassical time-dependent Hartree approximation [37]. The nuclear mean-field wave packet is replaced by an ensemble of classical trajectories propagating under the influence of the self-consistent potential

$$U^{\text{SCP}} = \langle \psi^{\text{elec}} | H | \psi^{\text{elec}} \rangle_{\mathbf{r}}. \quad (4)$$

The electronic mean-field Schrödinger equation becomes

$$i\hbar \frac{\partial}{\partial t} \phi^{\text{elec}} = \langle H \rangle_{\text{nuclear ensemble}} \phi^{\text{elec}}(\mathbf{r}, t). \quad (5)$$

This treatment neglects important correlations between electronic and nuclear motion. A better starting point than (1) is a multiconfigurational wave packet [20, 42–45]. A wave packet in a multielectronic-state molecular system may be written

$$\Psi = \sum_{\text{states } \alpha} c_{\alpha}(t) \phi_{\alpha}^{\text{elec}}(\mathbf{r}, \mathbf{R}(t)) \psi_{\alpha}^{\text{nuc}}(\mathbf{R}, t), \quad (6)$$

where $\phi_{\alpha}^{\text{elec}}$ is a normalized component of the electronic wave function, $\psi_{\alpha}^{\text{nuc}}$ is a normalized component of the nuclear-motion wave packet, and c_{α} is a time-dependent coefficient.

To improve upon the mean-field approximation in the semiclassical treatment, we add correlation by making the independent-trajectory approximation [15, 40]. (A quantum wave packet analog is the “independent first generation” approximation [45].) This replaces (5) by

$$i\hbar \frac{\partial}{\partial t} \phi^{\text{elec}} = H(\mathbf{R}(t)) \phi^{\text{elec}}(\mathbf{r}, \mathbf{R}, (t)) \quad (7)$$

for each trajectory. The combination of the independent-trajectory approximation and the semiclassical time-dependent Hartree approximation is called the semiclassical Ehrenfest approximation [23, 26–30].

Next we choose an electronic basis

$$\phi^{\text{elec}} = \sum_{\alpha} c_{\alpha}(t) \phi_{\alpha}^{\text{el}}(r, \mathbf{R}(t)), \quad (8)$$

where c_{α} is a coefficient, and $\phi_{\alpha}^{\text{el}}$ is an antisymmetrized many-electron configuration state function in either the adiabatic [8] or a diabatic [26] representation. Furthermore we make the semiclassical replacement

$$\frac{\partial \phi_{\alpha}^{\text{el}}}{\partial t} = \frac{d\mathbf{R}}{dt} \frac{\partial \phi_{\alpha}^{\text{el}}}{\partial \mathbf{R}}. \quad (9)$$

Substituting (8) and (9) into (7) yields the following time-dependent Schrödinger equation for the coefficients along the trajectory [20]

$$i\hbar \frac{\partial c_{\alpha}}{\partial t} = \sum_{\beta} c_{\beta}(t) \left[-i\hbar \dot{\mathbf{R}} \cdot \mathbf{d}_{\alpha\beta} + U_{\alpha\beta}(\mathbf{R}(t)) \right], \quad (10)$$

where

$$U_{\alpha\beta} \equiv \langle \phi_{\alpha}^{\text{el}} | H_{\text{elec}} | \phi_{\beta}^{\text{el}} \rangle_{\mathbf{r}} \quad (11)$$

and

$$\mathbf{d}_{\alpha\beta} \equiv \langle \phi_{\alpha}^{\text{el}} | \nabla_{\mathbf{R}} | \phi_{\beta}^{\text{el}} \rangle_{\mathbf{r}}. \quad (12)$$

In (12), H_{elec} is the so called electronic Hamiltonian, which also includes nuclear repulsion. It is defined by

$$H_{\text{elec}} = H - T_{\mathbf{R}}, \quad (13)$$

where $T_{\mathbf{R}}$ is the nuclear kinetic energy. Since $\mathbf{d}_{\alpha\beta}$ is anti-Hermitian, its diagonal elements vanish identically. Note that if an adiabatic representation is used in (8), \mathbf{U} is diagonal [13b], whereas if a diabatic representation is used in (8), $\mathbf{d}_{\alpha\beta}$ is assumed to be negligible and is neglected. The diagonal elements of \mathbf{U} are called potential energy surfaces, and U_{ii} is often denoted as V_i . In well established but somewhat inconsistent conventions, the off-diagonal elements of \mathbf{U} are called the diabatic couplings, and $\mathbf{d}_{\alpha\beta}$ is called the nonadiabatic coupling. It is convenient to reformulate (10) in terms of the reduced electronic density matrix, which is defined by its matrix elements as follows:

$$\rho_{\alpha\beta} \equiv c_{\alpha}c_{\beta}^*. \quad (14)$$

Substituting (14) into (10) yields a unitary Liouville-von Neumann equation [46], which in our case can be written as:

$$i\hbar \frac{\partial \rho_{\alpha\beta}}{\partial t} = - \sum_{\gamma} \left(\left[-i\hbar \dot{\mathbf{R}} \cdot \mathbf{d}_{\gamma\beta} + U_{\gamma\beta} \right] \rho_{\alpha\gamma} - \{\text{permute indices}\} \right). \quad (15)$$

Equation (15) is also called a unitary quantum Liouville equation. It is the quantum mechanical analog of Liouville's theorem in classical mechanics, and it is equivalent to the time-dependent Schrödinger equation [47, 48].

In the semiclassical Ehrenfest method one solves the coupled quantum mechanical equation (15) [or the equivalent equation (10)] for the electrons and simultaneously the classical equations of motion with the effective potential of equation (4) for the nuclear motion. Because we made the independent trajectory approximation, we repeat this calculation for an ensemble of initial conditions in the classical phase space (which may be sampled classically [11, 12] or quasiclassically [9, 10, 12a]), we average over initial conditions, and we sum over final states. The semiclassical Ehrenfest method shares with the exact solution of the Schrödinger equation that the results are independent of the representation (adiabatic, diabatic, or intermediate) used for the quantum subsystem. In fact this is true for each individual trajectory, not just for the ensemble average. But there is a serious defect in this method, namely that the system ends in an unphysical final state. Consider, for example, a collision or a photodissociation event where the final state is a diatomic molecule AB and an atom C. Suppose that the total energy is 2.5 eV above the classical potential energy of ground-state products, and that the products have one excited electronic state with an electronic excitation energy of 2.0 eV. The accurate quantum mechanical distribution of nuclear-motion energies will be bimodal: systems in the ground-electronic state will have 2.5 eV of nuclear energy, and systems in the excited electronic state will have 0.5 eV of nuclear energy. One might, under certain circumstances, even find a 50:50 distribution of these states. However, because a semiclassical Ehrenfest trajectory propagates on an average potential energy surface (4), it might end with an average nuclear energy of 1.25 eV or 1.5 eV (or in fact any energy in the range 0–2.5 eV), rather than being restricted to one of the two quantally allowed values.

Why is the semiclassical Ehrenfest method wrong? Because $\rho_{\alpha\beta}$ fails to tend to $\delta_{\alpha\beta}$ (a Kronecker delta) as $t \rightarrow \infty$. And why does that failure occur? Because (10) and (15), being equivalent to the time-dependent Schrödinger equation, are wrong for a subsystem.

There is only one system governed by the Schrödinger equation, namely the entire universe. All other systems are subsystems and satisfy a quantum master equation, in particular, a nonunitary Liouville-von Neumann equation with dissipation and dephasing. In our example of non-Born–Oppenheimer trajectories, the nuclei serve as a “bath” or “environment” for the electronic subsystem [30, 49–53]. To understand the effect of this bath, consider the wave packet of (6). In our example, there are two electronic states, corresponding to $\alpha = 1$ and $\alpha = 2$. The component of the nuclear wave packet corresponding to the lower-energy electronic state ($\alpha = 1$) moves faster, as does the trajectory subensemble corresponding to this subpacket. Therefore the two terms in (6) get out of phase, and they become subpackets in different regions of space; for these reasons their overlap tends to zero. As a consequence, $\rho_{\alpha\beta} \rightarrow 0$.

When a semiclassical Ehrenfest trajectory finishes a non-Born–Oppenheimer event, $\rho_{\alpha\beta}$ for $\alpha \neq \beta$ is not zero and $\rho_{\alpha\alpha}$ is neither zero nor unity. That is, the trajectory does not decohere to a pure state. Physically, dephasing would cause the off-diagonal elements to decay

$$\begin{pmatrix} \rho_{\alpha\beta} & \rho_{\alpha\beta} \\ \rho_{\beta\alpha} & \rho_{\beta\beta} \end{pmatrix} \rightarrow \begin{pmatrix} \rho'_{\alpha\alpha} & 0 \\ 0 & \rho'_{\beta\beta} \end{pmatrix}. \quad (16)$$

Algorithmically, we want our statistical ensemble of trajectories to “demix” to an ensemble of trajectories with quantized electronic states, schematically

$$\begin{pmatrix} \rho'_{\alpha\alpha} & 0 \\ 0 & \rho'_{\beta\beta} \end{pmatrix} \rightarrow \rho'_{\alpha\alpha} \begin{pmatrix} 1 & 0 \\ 0 & 0 \end{pmatrix} + \rho'_{\beta\beta} \begin{pmatrix} 0 & 0 \\ 0 & 1 \end{pmatrix}. \quad (17)$$

To achieve this we add algorithmic decay to the unitary Liouville-von Neumann equation such that each trajectory, at any given time, decoheres toward a given state, called the “decoherent state,” in such a way that the distribution of states (averaged over an ensemble of trajectories) is self-consistent with the density matrix. The resulting nonunitary Liouville-von Neumann equation, also called a quantum master equation, has the form

$$\frac{d\rho_{\alpha\beta}}{dt} = \left[\frac{d\rho_{\alpha\beta}}{dt} \right]_{\text{unitary}} + \left[\frac{d\rho_{\alpha\beta}}{dt} \right]_{\text{decoherent}}, \quad (18)$$

where the first term on the right-hand side is from (15) and generates dynamics equivalent to the Schrödinger Equation, and the second term is an algorithmic control term added to simulate the effect of decoherence. Both terms conserve total energy and total angular momentum of the combined quantal and classical subsystems. However energy is transferred between the two subsystems; when energy is transferred from the quantal subsystem to the classical one, this may be considered to be a form of dissipation.

The density matrix of (18) is a reduced density matrix, that is, a density matrix of a subsystem traced over its environment. In the present case, it is the electronic density matrix obtained by tracing over the nuclear degrees of freedom. This matrix, being Hermitian, can be diagonalized in any basis. In which basis does it become diagonal and stay diagonal? That basis is called the pointer basis [54], and the selection of this basis by the decoherent process is called environment-induced superselection or einselection [55]. The pointer basis is determined by the interaction of the subsystem with its environment; this interaction is sometimes called the measuring process. For example if the system is a spin- $\frac{1}{2}$ particle ($S = \frac{1}{2}$), and its interaction is to encounter a detector properly designed to measure S_z , the pointer basis will be the eigenvectors of the operator \hat{S}_z . If, however, the interaction with the environment is to encounter a detector properly designed to measure S_x , the pointer basis will be the eigenvector of \hat{S}_x . More generally, if the subsystem behaves adiabatically (such as when the frequencies of the environment are much lower than those of the subsystem), the pointer basis will be the adiabatic energy states of the subsystem [56], which is fully in accord with intuition. In the limit where the self-Hamiltonian is negligible compared to the subsystem-environment interaction, the eigenvectors of the interaction becomes the pointer state [57]. In the general case the pointer basis is unknown. The analog of the pointer basis in our algorithm is the basis used to express the decoherent states; we may call this the algorithmic pointer basis. Since the physical pointer basis is not easy to predict and may change with time as the system explores different regions of nuclear configuration space (i.e., as the electronic subsystem explores different aspects of its nuclear environment), our goal is to find an algorithm whose accuracy does not depend strongly on the choice of algorithmic pointer basis. In practice this means we seek an algorithm that yields good results in both the adiabatic and diabatic representations. Not only must we choose an algorithmic pointer basis, we must also choose the decoherent state, which will be labeled K . Thus $\alpha = K$ for the state toward which the system is decohering at a particular time along a particular trajectory.

To derive a form for the second term of (18) we make the reasonable assumption that $\text{Re } c_\alpha$ and $\text{Im } c_\alpha$ (in (10)) decay by a pure first-order process at the same rate in the algorithmic pointer basis [23]; this conserves the electronic phase angle, that is, it conserves $\arctan(\text{Im } c_\alpha / \text{Re } c_\alpha)$. Then we obtain, for example for the $\alpha\beta = \alpha K$ element [27]

$$\left(\frac{d\rho_{\alpha K}}{dt}\right)_{\text{decoherent}} = \frac{1}{2} \left[\frac{1}{\rho_{KK}} \left(\sum_{\gamma \neq K} \frac{\rho_{\gamma\gamma}}{\tau_{K\gamma}} \right) - \frac{1}{\tau_{\alpha K}} \right] \rho_{\alpha K}. \quad (19)$$

The more common assumption is that the master equation is linear, which yields:

$$\left(\frac{d\rho_{\alpha\beta}}{dt}\right)_{\text{decoherent}} = -\frac{1}{\tau_{\alpha\beta}} \rho_{\alpha\beta}, \quad \alpha \neq \beta. \quad (20)$$

To which state does the system decohere? We determine this stochastically by Tully's [17] fewest switches algorithm, which was originally proposed for use in surface hopping calculations. Trajectory surface hopping calculations [13, 16–18] stochastically switch the state in which the system propagates (i.e., the potential energy surface governing nuclear motion) to keep the ensemble of nuclear trajectories as consistent as possible with the quantal evolution of the quantal subsystem governed by the unitary Liouville-von Neumann equation. In contrast, our algorithm [29, 30] stochastically switches the decoherent state to keep the nuclear ensemble consistent with the unitary Liouville-von Neumann equation over each passage through a strong interaction of the electronic states, which is called *coherent switching*. At the same time the nuclei propagate on a potential energy surface consistent with the nonunitary Liouville-von Neumann equation incorporating *decay of mixing*. The algorithm is therefore called coherent switches with decay of mixing (CSDM). Because the boundaries of the coherent switching regions introduce time nonlocality, the algorithm is non-Markovian.

In summary, the CSDM algorithm introduces decoherence into the electronic reduced density matrix such that in the strong interaction region the potential energy surface governing nuclear motion has the desirable (representation-independent) properties of the semiclassical Ehrenfest potential, whereas in the asymptotic or weakly coupled regions the effective potential reduces to that of the decoherent state in the pointer basis. But the decoherent state switches stochastically in a coherent way for each complete passage through a strong interaction region. Thus we evolve two density matrices, one (evolved with decay of mixing) controls the effective potential energy surface for nuclear motion, and the other (evolved coherently through strong-interaction regions) controls stochastic switching of the decoherent state.

The decoherence process is first-order with rate constant τ^{-1} . For example, for a diagonal element $\rho_{\alpha\alpha}$ of the density matrix, with $\alpha \neq K$, we have

$$\frac{d\rho_{\alpha\alpha}}{dt} = \left(\frac{d\rho_{\alpha\alpha}}{dt} \right)_{\text{unitary}} - \frac{\rho_{\alpha\alpha}}{\tau_{\alpha K}}, \quad (21)$$

where the first term on the right is associated with coherent Ehrenfest propagation and the second term causes demixing. There are similar equations for other density matrix elements, except that they are nonlinear for off-diagonal elements $\rho_{\alpha\beta}$. We call τ the decoherence time or the demixing time.

Since our algorithmic demixing is analogous to but not identical to physical decoherence, it is reasonable that our demixing time should be similar to but not identical to the physical decoherence time. We therefore base our choice of the demixing time on three principles:

1. The semiclassical limit of a wave function is the sum of WKB-like trajectories associated with minimum wave packets, and decoherence of the superposition is faster than decoherence of the individual packets [57]. Nuclear wave packets move at different speeds on different surfaces, causing

dephasing and decay of overlap, and this leads to decay of off-diagonal elements of the density matrix [53].

2. The pointer basis is the one in which decoherence is fastest [57].
3. Decoherence slows down when the momentum component in the nonadiabatic coupling direction is small [29].

Using the first two principles we derived [53] an approximate expression for the physical decoherence rate constant for electronically nonadiabatic chemistry:

$$\frac{1}{\tau} = \frac{1}{\tau^{\Delta F}} + \sqrt{\left(\frac{1}{\tau^{\Delta p}}\right)^2 + \left(\frac{1}{\tau^{\Delta F}}\right)^2}, \quad (22)$$

where $\tau^{\Delta p}$ is a complicated expression associated with the wave packet having different momenta p_α and p_β on two surfaces V_α and V_β , and $\tau^{\Delta F}$ is a complicated expression associated with the wave packet experiencing different forces on the two surfaces. For parallel surfaces in one dimension,

$$\tau = \tau^{\Delta p} = \frac{\hbar}{|V_\alpha - V_\beta|} \sqrt{\frac{4\pi^2 |p_\alpha - p_\beta|}{\bar{p}}}, \quad (23)$$

where \bar{p} is the average momentum. The first factor (“prefactor”) on the right-hand side of (23) is the fastest time scale in the system.

For our purposes, the “correct” rate of algorithmic demixing is whatever makes the ensemble average with the *independent-trajectory approximation* best simulate the rate of change of populations and final-state distributions. We found that the following works well

$$\tau = \frac{\hbar}{|V_\alpha - V_\beta|} \left(1 + \frac{E_0}{(\mathbf{p} \cdot \hat{s})^2 / 2\mu} \right), \quad (24)$$

where \mathbf{p} is nuclear momentum, \hat{s} is the direction of the nonadiabatic coupling, μ is the nuclear reduced mass (\mathbf{p} and μ both correspond to iso-inertial coordinates scaled to a single reduced mass), and E_0 is a parameter that we set equal to 0.1 hartree. The final factor in (24) is motivated by principle no. 3 above and by the fact [55] that the fastest time scale in the system provides a lower bound on the physical decoherence time. Although our experience indicates that the performance of (24) can be improved by making the prefactor larger, we find that with the current form the results are reasonably insensitive to E_0 and that (24) works well for a diverse set of non-Born–Oppenheimer processes [29, 30].

Two further issues need to be considered. First is the direction of decoherent energy release and decoherent energy uptake (these energy exchanges are required because the potential energy surface is self-consistent with the decohering density matrix). We formulated the decoherence term such that the direction of the nuclear momentum in which energy is exchanged as the

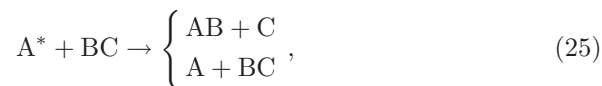
system decoheres (as the pointer state is einselected) is the direction of the nonadiabatic coupling vector when nonadiabatic coupling is large and is in the direction of the vibrational momentum when the nonadiabatic coupling is small. The latter is motivated by the existence of a “small” but nonremovable component of the nonadiabatic coupling associated with any motion of the nuclei [26].

The final issue to be considered is the criterion for a strong coupling region over which the density matrix that controls stochastic switching evolves coherently. For calculations in the adiabatic representation we take the boundaries of strong-coupling regions as the minima of the magnitude of the nonadiabatic coupling. For calculations in the diabatic representation, we take these boundaries as the minima of the diabatic level spacing (gap); using the maximum gap turned out to be slightly less accurate on average. At boundaries between strong-coupling regions, the switch-controlling coherent density matrix is synched to the relaxing one that controls the effective potential. This key element of the method differs from all previous trajectory surface hopping and decoherence algorithms; as a result the amount of decoherence introduced at strong-interaction-region boundaries depends on the length of the strong coupling region and the relaxation rates controlled by the decoherence times.

We emphasize that the DM potential energy surface switches gradually and smoothly between the various electronic surfaces; no hops are invoked, and therefore no frustrated hops arise. In the DM formalism, we preserve Ehrenfest-like motion in strong interaction regions or when the decay times are long. In the limit of short decay times, the DM formalism is similar to surface hopping in having instantaneous decay of the reduced density matrix, but surface hopping has no synching.

3 Tests

We validated the CSDM method for a variety of test cases for which we computed [58–60] accurate quantum mechanical transition probabilities by methods developed earlier [61] for converged quantum mechanical scattering theory. All of the test systems have the form



where * denotes electronic excitation; A, B, and C are atoms; and the collision occurs in full three-dimensional space with total angular momentum zero. The masses of the atoms in atomic mass units are denoted m_A , m_B , and m_C . The full set of tests are presented in [29, 30], and here I give only a survey of the results of those studies.

First we consider a case with $m_A = 10$, $m_B = 1.00783$, $m_C = 6$, and a potential energy surface resembling that for $\text{Br}^* + \text{H}_2$. This is a case of weakly

coupled surfaces that do not cross in either representation; the gap between the adiabatic surfaces is about 0.36 eV throughout the whole important region, and the diabatic coupling is a constant, 0.20 eV [59]. Table 1 shows results for a case with a total energy of 1.10 eV where the initial vibrational and rotational quantum numbers of BC are respectively $v = 0, j = 6$. In the table, P_R denotes the probability of reaction (top product in (25)), and P_Q is the probability of nonreactive quenching (electronic-to-vibrational energy transfer; bottom product in (25)). Table 1 shows the actual calculated probabilities, and Table 2 shows the dependence on representation.

Tables 1 and 2 show that trajectory surface hopping has a very strong dependence on representation. In simple cases like this weakly coupled atom-diatom collision, it is not too difficult to recognize which representation provides a better description (in this case it is the adiabatic one). However, for systems with complex potential energy surfaces, it is not always possible to know which representation is more appropriate [22]. There may be systems with some initial conditions for which the adiabatic representation is more accurate and other initial conditions for which the diabatic representation is

Table 1. Test results for a weakly coupled case

method	representation	P_Q	P_R
Trajectory surface hopping methods			
Parlant-Gislason (PG) ^a	adiabatic	0.01	0.002
	diabatic	0.55	0.359
Tully's fewest switches ^b	adiabatic	0.18	0.025
	diabatic	0.40	0.161
Fewest switches with time uncertainty ^c	adiabatic	0.18	0.015
	diabatic	0.33	0.044
Self-Consistent-potential methods			
Semiclassical Ehrenfest (SE)	either	0.003	0.000
CSDM	adiabatic	0.15	0.021
	diabatic	0.18	0.012
Accurate			
Quantum scattering	either	0.14	0.26

^aMethod of [16]

^bOriginal TFS+ method of [17] with frustrated hops ignored

^cFSTU gradV method of [24] and [25]

Table 2. Representation dependence for the weakly coupled case of Table 1

type of methods	method	P (diabatic)/ P (adiabatic) or P (adiabatic)/ P (diabatic)	Reaction
TSH	PG	55	180
	TFS+	2.1	6
	FSTU gradV	1.8	3
SCP	SE	1.0	— ^a
	CSDM	1.2	1.7

^aCannot compute because no reaction was observed due to qualitatively incorrect Ehrenfest potentials in the reactive exit valley

more appropriate. Furthermore, and even more serious, is that for systems with complex coupled potential energy surfaces, there may be regions of configuration space where the diabatic representation is more suitable and other regions or product valleys where the adiabatic representation is more suitable. Thus it may not be possible to find a good zero-order description that remains valid for a whole trajectory; this was one of the original motivations for trying to incorporate the representation independence of the semiclassical Ehrenfest method into our scheme. Tables 1 and 2 do show that the results obtained by the semiclassical Ehrenfest method are independent of representation; unfortunately though the results are too inaccurate to be useful. The CSDM method reduces the representation dependence to factors of 1.2 and 1.7 for the two probabilities, and the results are reasonably accurate in both representations, especially when we consider that the weak coupling case is especially difficult for semiclassical methods.

We carried out similar comparisons for additional test cases. In particular, we considered three kinds of systems, all of the form of (25) [28–30, 58–60]. We considered three cases of the weak coupling type already discussed, nine test cases with energetically accessible avoided crossings (where the diabatic potentials cross, but the adiabatic ones do not), and five test cases with energetically accessible conical intersections. The weak coupling cases include two strengths of diabatic coupling, one of which is studied with two different initial conditions. The avoided crossing cases consist of three different couplings (varying in strength and extent of delocalization), each studied with three different initial rotational states. The conical intersection cases correspond to five different coupling functions. The results [28–30] are shown in Table 3, which presents mean unsigned percentage errors in the probabilities of quenching and reaction, in the total nonadiabatic transition probability ($P_N \equiv P_Q + P_R$), and in the final internal energy distributions of the diatomic fragments. The means are computed by logarithmic averaging [62] so as to give equal weight to overestimates and underestimates, and the results are averaged over the diabatic and adiabatic calculations. The CSDM method leads to uniformly good results for all three kinds of systems. In fact the errors are comparable to the

Table 3. Mean unsigned percentage errors of semiclassical methods for non-Born–Oppenheimer trajectories tested against accurate quantal results for 17 test cases averaged over diabatic and adiabatic representations

kind of method	method	kind of system			averaged over kinds of systems
		weak coupling	avoided crossing	conical intersection	
TSH	PG	298	107	52	152
	TFS+	195	58	44	99
	FSTU gradV	74	40	44	53
SCP	SE	– ^a	65	55	–
	CSDM	24	21	31	25

^aCannot compute mean error because there is no reaction, and hence there are no reactive products for which to compute mean internal energies

accuracy attainable [21] by trajectory methods for single-surface problems of this nature.

4 Concluding Remarks

We have shown that decoherence is essential for modeling the quantum mechanical electronic subsystem in the simulation of electronically nonadiabatic chemical dynamics. We have developed an improved self-consistent-potential method called Coherent Switches with Decay of Mixing (CSDM) by writing the time derivative of each density matrix element as the sum of a coherent Ehrenfest-like term and a demixing term. The demixing terms control the decay of the system from a mixed state to a stochastically selected pure state called the decoherent state. The form of the equations was determined by requiring:

- Conservation of total energy and angular momentum;
- Conservation of electronic phase angle;
- The decoherent state switches to maintain self-consistency, but it is otherwise chosen as coherently as possible for each complete passage through a strong interaction region (corresponding to non-Markovian decoherence);
- The direction in which energy is exchanged between the classical vibrational degrees of freedom and the quantal electronic degrees of freedom as the system decoheres is chosen physically based on the nature of the nonadiabatic coupling.

The CSDM algorithm provides a semiclassical version of the multiconfigurational self-consistent-field method that puts mixed quantum/classical dynamics for non-Born–Oppenheimer systems on a comparable footing with BO dynamics. In particular the accuracy is comparable to that attainable when

trajectory methods are applied to single-surface problems. Furthermore the classical subsystem experiences no discontinuities in momenta, coordinates, or potentials, there is relatively little dependence on representation, and the cost of the calculation is similar to that for single-surface trajectories.

A key advantage of the semiclassical SCDM algorithm is that it is more practical than a fully quantal multiconfigurational quantum master equation [63–67] for applications to complex systems.

Acknowledgments

The work reviewed here was carried out in collaboration with Michael Hack, Ahren Jasper, Shikha Nangia, and Chaoyuan Zhu, and their contributions to all stages of the project are gratefully acknowledged. This work was supported in part by the National Science Foundation through grant no. CHE03-49122.

References

1. Gao J, Thompson MA (eds) (1998) Combined quantum mechanical and molecular mechanical methods. American Chemical Society, Washington
2. Gao J, Truhlar DG (2002) Quantum mechanical methods for enzyme kinetics. *Annu Rev Phys Chem* 53: 467–505
3. Lin H, Truhlar DG QM/MM: What have we learned, where are we, and where do we go from here? *Theor Chem Acc*, in press
4. Truhlar DG, Garrett BC (1980) Variational transition state theory. *Acc Chem Res* 13: 440–448
5. Truhlar DG, Isaacson AD, Garrett BC (1985) Generalized transition state theory. In: Baer M (ed) *Theory of chemical reaction dynamics*. CRC Press, Boca Raton, Vol. 4, pp. 65–137
6. Guo Y, Thompson DL (1998) A multidimensional semiclassical approach for treating tunneling within classical trajectory simulations. In: Thompson DL (ed) *Modern methods for multidimensional dynamics calculations in chemistry*. World Scientific, Singapore, pp. 713–737
7. Marx D, Hutter J (2000) *Ab initio* molecular dynamics: theory and implementation. In: Grotendorst J (ed) *Modern methods and algorithms of quantum chemistry*. John von Neuman Institute for Computing, Jülich, pp. 329–477
8. Born M, Haug K (1954) *The dynamical theory of crystal lattices*. Oxford University Press, London
9. Truhlar DG, Muckermann JT (1979) Reactive scattering cross sections: Quasiclassical and semiclassical methods. In: Bernstein RB (ed) *Atom-molecule collision theory*. Plenum, New York pp. 505–566
10. Raff LM, Thompson DL (1985) The classical trajectory approach to reactive scattering. In: Baer M (ed) *Theory of chemical reaction dynamics*. CRC Press, Boca Raton, Vol. 3, pp. 1–121
11. Rapoport DC (1995) *The art of molecular dynamics simulation*. Cambridge University Press, Cambridge

12. (a) Schatz GC, Horst M, Takayanagi T (1998) Computational methods for polyatomic bimolecular reactions. In: Thompson DL (ed) *Modern methods for multidimensional dynamics calculations in chemistry*. World Scientific, Singapore, pp. 1–33. (b) Benjamin I, Molecular dynamics methods for studying liquid interfacial phenomena. In: Thompson DL (ed) *Modern methods for multidimensional dynamics calculations in chemistry*. World Scientific, Singapore, pp. 101–142. (c) Bolton K, Hase WL, Peslherbe GH, Direct dynamics simulations of reactive systems. In: Thompson DL (ed) *Modern methods for multidimensional dynamics calculations in chemistry*. World Scientific, Singapore, pp. 143–189. (d) Stanton RV, Miller JL, Kollman DA, Macromolecular dynamics, In: Thompson DL (ed) *Modern methods for multidimensional dynamics calculations in chemistry*. World Scientific, Singapore, pp. 355–383. (e) Brady JW, Molecular dynamics simulations of carbohydrate solvation. In: Thompson DL (ed) *Modern methods for multidimensional dynamics calculations in chemistry*. World Scientific, Singapore, pp. 384–400. (f) Rice BM, Molecular simulations of detonation. In: Thompson DL (ed) *Modern methods for multidimensional dynamics calculations in chemistry*. World Scientific, Singapore, pp. 472–528
13. (a) Tully JC, Preston RK (1971) Trajectory surface hopping approach to nonadiabatic molecular collisions: the reaction of H^+ with D_2 . *J Chem Phys* 55: 562–572. (b) Truhlar DG, Duff JW, Blais NC, Tully JC, Garrett BC (1982) The Quenching of $Na(3^2P)$ by H_2 : Interactions and dynamics. *J Chem Phys* 77: 764–766. (c) Blais, NC, Truhlar DG (1983) Trajectory-surface-hopping study of $Na(3p^2P) + H_2 \rightarrow Na(3s^2S) + H_2(v', j', \theta)$. *J Chem Phys* 79: 1334–1342
14. Meyer HD, Miller WH (1979) A classical analog for electronic degrees of freedom in nonadiabatic collision processes. *J Chem Phys* 70: 3214–3223
15. Micha DA (1983) A self-consistent eikonal treatment of electronic transitions in molecular collisions. *J Chem Phys* 78: 7138–7145
16. Parlant G, Gislason EA (1989) An exact trajectory surface hopping procedure: comparison with exact quantal calculations. *J Chem Phys* 91: 4416–4418
17. Tully JC (1990) Molecular dynamics with electronic transitions. *J Chem Phys* 93: 1061–1071
18. Chapman S (1992) The classical trajectory–surface hopping approach to charge-transfer processes. *Adv Chem Phys* 82: 423–483
19. Muller U, Stock G (1997) Surface-hopping modeling of photoinduced relaxation dynamics on coupled potential-energy surfaces. *J Chem Phys* 107: 6230–6245
20. Tully JC (1998) Nonadiabatic dynamics. In: Thompson DL (ed) *Modern methods for multidimensional dynamics calculations in chemistry*, World Scientific, Singapore, pp. 34–72
21. Topaler MS, Allison TC, Schwenke DW, Truhlar DG (1998) What is the best semiclassical method for photochemical dynamics in systems with conical intersections? *J Chem Phys* 109: 3321–3345, (1999) 110: 687–688(E), (2000) 113: 3928(E)
22. Hack MD, Truhlar DG (2000) Semiclassical trajectories at an exhibition. *J Phys Chem A* 104: 7917–7926
23. Hack MD, Truhlar DG (2001) A natural decay of mixing algorithm for non-Born Oppenheimer trajectories. *J Chem Phys* 114: 9305–9314
24. Jasper AW, Stechmann SN, Truhlar DG (2002) Fewest switches with time uncertainty: A modified trajectory surface hopping algorithm with better accuracy for classically forbidden electronic transitions. *J Chem Phys* 116: 5424–5431, 117: 1024(E)

25. Jasper AW, Truhlar DG (2003) Improved treatment of momentum at classically forbidden electronic transitions in trajectory surface hopping calculations. *Chem Phys Lett* 369: 60–67
26. Jasper AW, Kendrick BK, Mead CA, Truhlar DG (2004) Non-Born–Oppenheimer chemistry: Potential surfaces, couplings, and dynamics. *Adv Ser Phys Chem* 14: 329–391
27. Zhu C, Jasper AW, Truhlar DG (2004) Non-Born–Oppenheimer trajectories with self-consistent decay of mixing. *J Chem Phys* 120: 5543–5557
28. Jasper AW, Zhu C, Nangia S, Truhlar DG (2004) Introductory lecture: Nonadiabatic effects in chemical dynamics. *Discuss Faraday Soc* 127: 1–22
29. Zhu C, Nangia S, Jasper AW, Truhlar DG (2004) Self-consistent decay of mixing and trajectory surface hopping with coherent complete passages. *J Chem Phys* 121: 7658–7670
30. Zhu C, Jasper AW, Truhlar DG (2005) Non-Born–Oppenheimer Liouville–von Neumann dynamics. Evolution of a subsystem controlled by linear and populations-driven decay of mixing with decoherent and coherent switching. *J Chem Theory Comput* 1: 527–540
31. Stock G, Thoss M (2005) Classical description of nonadiabatic quantum dynamics. *Adv Chem Phys* 131: 243–375
32. Rapp D, Sharp TE (1963) Vibrational energy transfer in molecular collisions involving large transition probabilities. *J Chem Phys* 38: 2641–2648
33. Sharp TE, Rapp D (1965) Evaluation of approximations used in the calculation of excitation by collision. I. Vibrational excitation of molecules. *J Chem Phys* 43: 1233–1244
34. Muckermann JT, Rusinek I, Roberts RE, Alexander M (1976) Probabilities for classically forbidden transitions using classical and classical path methods. *J Chem Phys* 65: 2416–2428
35. Billing Sorensen G (1974) Semiclassical three-dimensional inelastic scattering theory. *J Chem Phys* 61: 3340–3343
36. Gentry WR (1979) Vibrational excitation II: classical and semiclassical methods. In Bernstein RB (ed) *Atom-molecule collision theory*. Plenum, New York, pp. 391–425
37. Gerber RB, Buch V, Ratner MA (1982) Time-dependent self-consistent field approximation for intramolecular energy transfer. I. Formulation and application to dissociation of van der Waals molecules. *J Chem Phys* 77: 3022–3030
38. Halcomb LL, Diestler DJ (1985) Dynamics of vibrational predissociation of van der Waals molecules. In: Numrich RW (ed) *Supercomputer applications*. Plenum, New York, pp. 273–288
39. Billing GD (1987) Rate constants for vibrational transitions in diatom-diatom collisions. *Comput Phys Commun* 44: 121–136
40. Garcia-Vela A, Gerber RB, Imre DG (1992) Mixed quantum wave packet/classical trajectory treatment of the photodissociation process $\text{ArHCl} \rightarrow \text{Ar} + \text{H} + \text{Cl}$. *J Chem Phys* 97:7242–7250
41. Han H, Brumer P (2005) Decoherence effects in reactive scattering. *J Chem Phys* 122: 144316/1–8
42. Sawada S, Metiu H (1986) A multiple trajectory theory for curve crossing problems obtained by using a Gaussian wave packet representation of the nuclear motion. *J Chem Phys* 84: 227–238
43. Meyer H-D, Manthe U, Cederbaum LS (1990) The multi-configurational time-dependent Hartree approximation. *Chem Phys Lett* 165: 73–78

44. Kotler Z, Neria E, Nitzan A (1991) Multi-configurational time-dependent self-consistent-field approximations in the numerical solution of quantum dynamical problems. *Comput Phys Commun* 63: 234–258
45. Hack MD, Wensmann AM, Truhlar DG, Ben-Nun M, Martinez TJ (2001) Comparison of full multiple spawning, Trajectory surface hopping, and converged quantum mechanics for electronically nonadiabatic dynamics. *J Chem Phys* 115: 1172–1186
46. Neumann JV (1955) *Mathematical foundations of quantum mechanics*, Princeton University Press, Princeton [originally published in German in 1932: *Mathematische Grundlagen der Quantenmechanik*, Springer, Berlin Heidelberg New York]
47. Sakurai JJ (1985) *Modern quantum mechanics*. Addison-Wesley, Redwood City, CA p. 181
48. Gottfried K, Yan TM (2003) *Quantum mechanics: Fundamentals*. 2nd edn, Springer, Berlin Heidelberg New York, p. 64
49. Schwartz BJ, Bittner ER, Prezhdo OV, Rossky PJ (1996) Quantum decoherence and the isotope effect in condensed phase nonadiabatic molecular dynamics simulations. *J Chem Phys* 104: 5942–5955
50. Bittner ER, Rossky PJ (1995) Quantum decoherence in mixed quantum-classical systems: nonadiabatic processes. *J Chem Phys* 103: 8130–8143
51. Bittner ER, Rossky PJ (1997) Decoherent histories and nonadiabatic quantum molecular dynamics simulations. *J Chem Phys* 107: 8611–8618
52. Preszhdo OV, Rossky PJ (1997) Evaluation of quantum transition rates from quantum-classical molecular dynamics simulations. *J Chem Phys* 107: 5863–5878
53. Jasper AW, Truhlar DG (2005) Electronic decoherence time for non-Born–Oppenheimer trajectories. *J Chem Phys* 123: 64103/1–4
54. Zurek WH (1981) Pointer basis of quantum apparatus: Into what mixture does the wave packet collapse? *Phys Rev D* 24: 1516–1525
55. Zurek WH (2003) Decoherence, einselection, and the quantum origins of the classical. *Rev Mod Phys* 75: 715–775
56. Paz JP, Zurek H (1999) Quantum limit of decoherence: environment induced superselection of energy eigenstates. *Phys Rev Lett* 82: 5181–5185
57. Paz JP, Habib S, Zurek WH (1993) Reduction of the wave packet: preferred observable and decoherence time scale. *Phys Rev D* 47: 488–501
58. Volobuev YL, Hack MD, Topaler MS, Truhlar DG (2000) Continuous surface switching: An improved time-dependent self-consistent-field method for nonadiabatic dynamics. *J Chem Phys* 112: 9716–9726
59. Jasper AW, Hack MD, Truhlar DG (2001) The treatment of classically forbidden electronic transitions in semiclassical trajectory surface hopping calculations. *J Chem Phys* 115: 1804–1816
60. Jasper AW, Truhlar DG (2005) Conical intersections and semiclassical trajectories: Comparison to accurate quantum dynamics and analyses of the trajectories. *J Chem Phys* 122: 44101/1–16
61. (a) Staszewska G, Truhlar DG (1987) Convergence of L^2 methods for scattering problems. *J Chem Phys* 86: 2793–2804. (b) Schwenke DW, Haug K, Truhlar DG, Sun Y, Zhang JZH, Kouri DJ (1987) Variational basis-set calculations of accurate quantum mechanical reaction probabilities. *J Phys Chem* 91: 6080–6082. (c) Sun Y, Kouri DJ, Truhlar DG, Schwenke DW (1990) Dynamical basis sets for

- algebraic variational calculations in quantum mechanical scattering theory. *Phys Rev A* 41: 4857–4862. (d) Schwenke DW, Mielke SL, Truhlar DG. (1991) Variational reactive scattering calculations: computational optimization strategies. *Theoret Chim Acta* 79: 241–269. (e) Tawa GJ, Mielke SL, Truhlar DG, Schwenke DW (1994) Algebraic variational and propagation formalisms for quantum dynamics calculations of electronic-to-vibrational, rotational energy transfer and application to the quenching of the 3p state of sodium by hydrogen molecules. *J Chem Phys* 100: 5751–5777. (f) Tawa GJ, Mielke SL, Truhlar DG, Schwenke DW (1994) Linear algebraic formulation of reactive scattering with general basis functions. *Adv Mol Vib Coll Dyn* 2B: 45–116
62. Allison TC, Truhlar DG (1998) Testing the accuracy of practical semiclassical methods: Variational transition state theory with optimized multidimensional tunneling. In: Thompson DL (ed) *Modern methods for multidimensional dynamics calculations in chemistry*. World Scientific, Singapore, pp. 618–712
 63. Stock G (1995) Nonperturbative generalized master equation for the spin-boson problem. *Phys Rev E* 51: 3038–3044
 64. Pesce L, Saalfrank P (1998) The coupled channel density matrix method for open quantum systems: Formulation and application to the vibrational relaxation of molecules scattering from nonrigid surfaces. *J Chem Phys* 108: 3045–3056
 65. Pesce L, Gerdtts T, Manthe U, Saalfrank P (1998) Variational wave packet method for dissipative photodesorption problems. *Chem Phys Lett* 288: 383–390
 66. Burghardt I (2001) Reduced dynamics with initial correlations: multiconfigurational approach. *J Chem Phys* 114: 89–101
 67. Burghardt I, Nest M, Worth GA (2003) Multiconfigurational system-bath dynamics using Gaussian wave packets: energy relaxation and decoherence induced by a finite-dimensional bath. *J Chem Phys* 119: 5364–5378